

Cathodoluminescence imaging and spectroscopy of excited states in InAs self-assembled quantum dots

S. Khatsevich and D. H. Rich^{a)}

Department of Physics, Ilse Katz Center for Meso and Nanoscale Science and Technology, Ben-Gurion University of the Negev, P.O. Box 653, Beer-Sheva 84105, Israel

Eui-Tae Kim and A. Madhukar

Department of Materials Science and Engineering, Nanostructure Materials and Devices Laboratory, University of Southern California, Los Angeles, California 90089-0241

(Received 17 November 2004; accepted 21 April 2005; published online 20 June 2005)

We have examined state filling and thermal activation of carriers in buried InAs self-assembled quantum dots (SAQDs) with excitation-dependent cathodoluminescence (CL) imaging and spectroscopy. The InAs SAQDs were formed during molecular-beam epitaxial growth of InAs on undoped planar GaAs (001). The intensities of the ground- and excited-state transitions were analyzed as a function of temperature and excitation density to study the thermal activation and reemission of carriers. The thermal activation energies associated with the thermal quenching of the luminescence were measured for ground- and excited-state transitions of the SAQDs, as a function of excitation density. By comparing these activation energies with the ground- and excited-state transition energies, we have considered various processes that describe the reemission of carriers. Thermal quenching of the intensity of the QD ground- and first excited-state transitions at low excitations in the ~ 230 – 300 -K temperature range is attributed to dissociation of excitons from the QD states into the InAs wetting layer. At high excitations, much lower activation energies of the ground and excited states are obtained, suggesting that thermal reemission of single holes from QD states into the GaAs matrix is responsible for the observed temperature dependence of the QD luminescence in the ~ 230 – 300 -K temperature range. The dependence of the CL intensity of the ground- and first excited-state transition on excitation density was shown to be linear at all temperatures at low-excitation density. This result can be understood by considering that carriers escape and are recaptured as excitons or correlated electron-hole pairs. At sufficiently high excitations, state-filling and spatial smearing effects are observed together with a sublinear dependence of the CL intensity on excitation. Successive filling of the ground and excited states in adjacent groups of QDs that possess different size distributions is assumed to be the cause of the spatial smearing. © 2005 American Institute of Physics. [DOI: 10.1063/1.1935743]

I. INTRODUCTION

Self-assembled quantum dots (SAQDs) have been studied intensively both experimentally and theoretically due to their applications in optoelectronic devices such as quantum dot (QD) lasers¹ and infrared photodetectors^{2,3} and for their potential in the development of quantum nanodevices.^{4–6} An optimal operation of these devices would be difficult without a thorough understanding of the optical properties of SAQDs at different temperatures and excitations. Since most QD-based devices are intended to work at room temperature, an understanding of their behavior at high temperatures is of great importance. Quenching of the QD luminescence with increasing temperature is commonly attributed to the carrier thermal escape from the QDs to the InAs wetting layer (WL) and to the continuum of states in the GaAs barrier^{7–10} or nonradiative recombination centers.^{10–12} In spite of extensive studies, consensus has not yet been reached on whether the thermal reemission of excitons^{13–17} or free electrons and holes^{8,18} from dots into the barrier is responsible for the observed thermal quenching of the QD luminescence at high

temperatures. The influence of carrier excitation density on the subsequent optical properties of SAQDs, particularly the thermal quenching of the QD luminescence, has been largely neglected in past studies.^{8,19} A number of effects at low and high excitations that limit the use of QD devices are known. At low-excitation density, a suppressed relaxation from excited states, also known as the phonon bottleneck effect, limits the use of QD lasers for high-speed applications. This effect was predicted^{20,21} and observed recently in InAs QDs.^{22,23} At high-excitation densities, state-filling effects are well known from photoluminescence (PL) experiments and are commonly used to access the excited-state spectrum.^{23–25} Yet, only a few studies have been performed in which the excitation dependence of the QD luminescence intensity of the ground-^{18,26,27} and excited-state transitions was studied systematically at different temperatures and excitation conditions.^{8,17}

In this work we have examined the temperature and excitation dependence of the luminescence intensity of the ground- and excited-state transitions in InAs SAQDs with cathodoluminescence (CL) imaging and spectroscopy. We have performed a detailed analysis of CL emission obtained

^{a)}Electronic mail: danrich@bgumail.bgu.ac.il

at low- and high-excitation densities in the 230–300-K temperature range for five InAs QD samples. The thermal activation energies associated with the thermal quenching of the luminescence were measured for ground- and excited-state transitions of the SAQDs, as a function of excitation density. By comparing these activation energies with the ground- and excited-state transition energies, we have considered various processes that describe the reemission of carriers. All samples share the same SAQD growth and formation conditions prior to capping, but possess different electronic levels after capping due to the incorporation of a lateral potential confinement layer (LPCL) that is positioned at different layers of the QDs for each sample. A suppressed relaxation from the first excited state at low-excitation density and state-filling and spatial smearing effects at high excitations were observed for all InAs QD samples.

II. EXPERIMENTAL DETAILS

The self-assembled InAs QD samples were grown on undoped planar GaAs (001) substrates by solid-source molecular-beam epitaxy (MBE), as has been described previously.^{8,28} Briefly, InAs QDs were formed at a substrate temperature of 500 °C by depositing 2.5-monolayers (ML) of InAs at a rate of 0.054 ML/s under an As₄ partial pressure of 7×10^6 Torr. Subsequently, the samples were cooled to 350 °C for the growth of capping layers deposited by migration enhanced epitaxy. Two reference InAs QD samples were grown. The first was capped by 30-ML In_{0.15}Ga_{0.85}As followed by deposition of 140-ML GaAs while the second was capped solely by GaAs. In samples labeled 1, 2, and 3, 10 MLs of the 30-ML In_{0.15}Ga_{0.85}As were replaced by an In_{0.15}Al_{0.25}Ga_{0.60}As layer, which forms a LPCL. The LPCL is positioned at different heights of the QDs for each of samples 1–3. Sample 1 has the LPCL located at the bottom of the InAs QDs. In samples 2 and 3, the LPCL is positioned 10 and 20 MLs above the bottom of the QDs, respectively. Previous atomic force microscopy (AFM) results obtained from uncapped 2.5-ML InAs QDs showed that the QD density was $\sim 400/\mu\text{m}^2$, with the measured average QD width and height of ~ 20 and ~ 6 nm, respectively.²⁸

The CL experiments were performed with a modified JEOL-5910 scanning electron microscope (SEM) using a 15-keV electron beam with probe current in the 0.03–35-nA range.²⁹ An InP:InGaAs photomultiplier tube (PMT) operating in the 950–1700-nm spectral range was used to detect the luminescence dispersed by a 0.25-m monochromator. Measurements were conducted at different temperatures in the 50–300-K temperature range. In order to increase the range of accessible excitation densities, the excitation volume was varied by defocusing the electron beam in reproducible steps.³⁰ The respective spot area was measured by exposing an electron resist layer that is normally used for electron-beam lithography. In the very low excitation density regime, the electron beam was defocused to a circular spot with a diameter of 90 μm at the sample surface. For an electron beam of this diameter, the dose of exposure was found to be homogeneously distributed, within the sensitivity of the electron resist. In this way, the collected CL intensity and

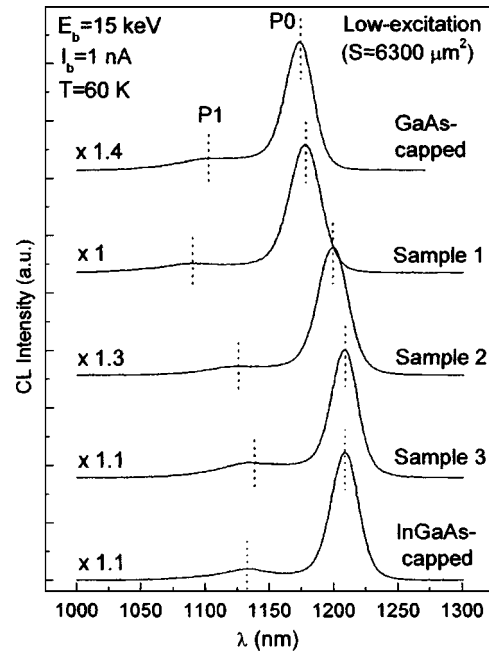


FIG. 1. Spatially averaged CL spectra of the GaAs- and the InGaAs-capped samples, and samples 1, 2, and 3 acquired at low excitation under a defocused e-beam condition for $T=60$ K. The ground-state (GS) and first excited-state peaks, labeled P0 and P1, respectively, are indicated by the vertical dashed lines.

measured photon count rates remain reasonable and provide an adequate signal-to-noise ratio. The defocusing approach permits measuring CL emission with an excitation density that is several orders of magnitude smaller than what can be employed using a focused electron beam.³⁰ This is made possible, owing to the excitation, e.g., of a large number of QDs $\sim 2.5 \times 10^6$, when the defocused spot size is 90 μm .

III. RESULTS AND DISCUSSIONS

A. Cathodoluminescence spectroscopy at different excitation densities

Figure 1 shows a low-excitation spatially averaged CL spectra of the GaAs and InGaAs-capped samples and samples 1, 2, and 3 acquired for a beam energy of 15 keV and beam current of 1 nA, while the electron beam was defocused to a spot size of $S=6300 \mu\text{m}^2$. In this very low excitation density regime, the steady-state average occupation in the QDs, n_{QD} , is well below one electron-hole pair per dot. The relationship between the carrier occupation number in the QDs, n_{QD} , and probe current, I_b , can be approximated by

$$n_{\text{QD}} \approx \frac{I_b E_b \tau_r L_D}{3e E_g V_e A_D}, \quad (1)$$

where E_b is the e-beam energy (15 keV), E_g is the GaAs band gap, which is 1.52 eV at $T \approx 50$ K, V_e is the e-h excitation volume at 15 keV, which is 3.4 and 9500 μm^3 for focused and defocused electron beams, respectively, L_D is the carrier diffusion length ($\sim 0.5 \mu\text{m}$), τ_r is the e-h lifetime (~ 0.5 ns),⁸ and A_D is the density of QDs ($400 \mu\text{m}^{-2}$).²⁸ Using the values appropriate for our experimental conditions, we get $n_{\text{QD}} \approx 3.8 I_b$ (nA) for a focused electron beam (the case of a high-excitation density), whereas for very low ex-

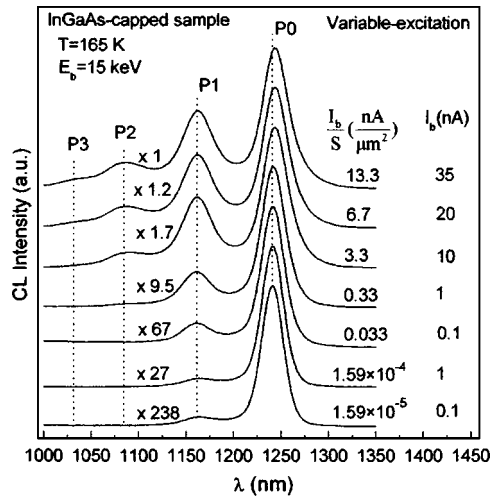


FIG. 2. Spatially averaged CL spectra for the InGaAs-capped sample acquired with a focused and strongly defocused electron beam at different probe currents I_b for $T=165$ K. The GS and three excited-state peaks, labeled P0 and P1–P3, respectively, are indicated by the vertical dashed lines. The lowest two spectra were acquired under low-excitation conditions (a defocused e-beam with spot area $S=6300 \mu\text{m}^2$) and beam currents of 0.1 and 1 nA, respectively.

citation densities in the defocused e-beam case (i.e., when $S=6300 \mu\text{m}^2$), $n_{\text{QD}} \approx 10^{-3} I_b$ (nA). From the results of the excitation-dependent CL spectroscopy (see Fig. 2), two peaks labeled P0 and P1 are identified as the ground-state (GS) and first excited-state transitions, respectively.

Similar results were obtained for all five samples with small differences in the CL peak positions, as shown in Fig. 1. We will therefore present mainly the results obtained for one sample, namely, the InGaAs-capped sample. Spatially averaged CL spectra of the InGaAs-capped sample at different excitation densities are shown in Fig. 2. The spectra were acquired for a beam energy of 15 keV at $T=165$ K. All the spectra are normalized to have nearly the same intensity; the scaling factors are indicated. The excitation current densities (shown in units of $\text{nA}/\mu\text{m}^2$) were varied from very low for a strongly defocused electron beam (the two lowest spectra in Fig. 2) to very high conditions when a focused electron beam was rastered over a $64 \times 48 \mu\text{m}^2$ region with various probe currents. On increasing the excitation density, the ratio between the intensity of the high- and low-energy peaks increases. Therefore, we assign four peaks, indicated by vertical dashed lines and labeled P0, P1, P2, and P3, to the GS and three excited-state transitions, respectively, which were observed in previous reports for similar InAs SAQDs.^{22,25,31}

Figures 1 and 2 show that the intensity of the first excited-state transition maintains $\sim 10\%$ of the intensity of the GS transition even for a vanishingly small average steady-state occupation well below one electron–hole pair per dot. We estimate from Eq. (1) that the four lowest CL spectra in Fig. 2, corresponding to the four lowest-excitation densities, have an average steady-state carrier population, n_{QD} , of 1×10^{-4} , 1×10^{-3} , 0.4, and 3.8, respectively. These results demonstrate a suppressed relaxation to the ground state in the low-density regime, which is the phonon bottleneck effect. A similar phonon bottleneck effect for InAs QDs was observed in a photoluminescence study using a weak excitation in which the first excited-state emission exhibited an intensity of $\sim 16\%$ of the ground-state emission intensity at a temperature of 7 K.²² Under high-excitation conditions, CL spectra in Fig. 2 show a well-defined ground-state and two excited-state transitions with energy spacings of 67 and 74 meV, consistent with previous measurements for similarly grown QD structures.^{22,25} An onset of the third excited-state transition, P3, is observed for the InGaAs-capped sample at beam currents above 20 nA. In the other samples, only two excited-state transitions are indicated. The measured ground- and excited-state transition energies E_0 , E_1 , and E_2 , as obtained from CL spectroscopy at $T=60$ K for the five QD samples, are summarized in Table I. $\Delta E_{10}=E_1-E_0$ and $\Delta E_{21}=E_2-E_1$ are intersublevel spacings between the GS and excited-state transitions. The ground- and excited-state transition energies of the InGaAs-capped sample are reduced by ~ 35 meV with respect to the transition energies of the GaAs-capped sample because of an overall lower confinement potential in the case of InGaAs capping.³² The transition energies of sample 1, with the LPCL located at the bottom of the InAs QDs, are close to the transition energies of the GaAs-capped sample. In the case of sample 3, with the LPCL located on top of the QDs, the transition energies are nearly identical with those of the InGaAs-capped sample. Further, the intersublevel spacing ΔE_{10} of sample 1 is increased by 20 meV relative to the intersublevel spacing of the InGaAs-capped sample, consistent with the results of previous PL and photoluminescence excitation (PLE) measurements.²⁸

B. Temperature- and excitation-dependent CL for low-excitation densities

CL spectra of the InGaAs-capped sample, acquired with a strongly defocused electron beam for a beam energy of 15 keV and beam current of 1 nA, are shown in Fig. 3. The

TABLE I. Ground- and excited state transition energies E_0 , E_1 , and E_2 obtained from CL spectroscopy at $T=60$ K for the QD samples used in this study. $\Delta E_{10}=E_1-E_0$ and $\Delta E_{21}=E_2-E_1$ are the QD intersublevel spacings.

	E_0 (eV)	E_1 (eV)	E_2 (eV)	ΔE_{10} (meV)	ΔE_{21} (meV)
Sample 1	1.052	1.139	1.212	87	73
Sample 2	1.034	1.105	1.180	71	75
Sample 3	1.026	1.093	1.168	67	75
InGaAs-capped	1.026	1.093	1.167	67	74
GaAs-capped	1.057	1.130	1.206	73	76

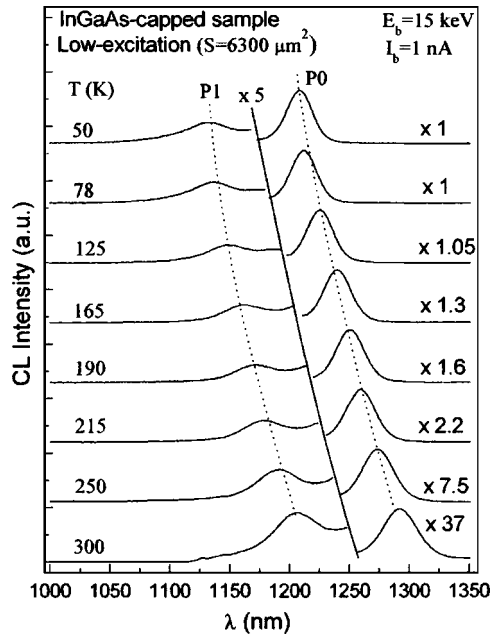


FIG. 3. Spatially averaged CL spectra for the InGaAs-capped sample acquired at low-excitation density in the $50 \leq T \leq 300$ K temperature range. The GS (P0) and first excited-state components (P1) are indicated. The left part of each spectrum containing peak P1 (and separated from the main peak P0 by a dashed line) was additionally multiplied by a factor of 5.

spectra were acquired for various temperatures in the 50–300-K temperature range. All the spectra are normalized to have nearly the same intensity, and scaling factors are indicated. In order to show that peak P1 of the first excited-state transition exists at all temperatures, revealing the suppressed relaxation from the first excited state in the low-excitation-density regime, we have multiplied the portion of each spectrum containing this peak by a factor of 5.

Spatially averaged CL intensities of the GS, P0, and excited-state transitions P1 and P2, which exhibit an Arrhenius behavior at low- and high-excitation densities, are shown in a log of CL intensity versus $1/kT$ plot in Fig. 4 for the InGaAs-capped sample. In order to estimate the activation energies of peaks P0, P1, and P2, we have performed linear fits of the log of intensity versus $1/kT$ data in the 230–300-K temperature range. The solid lines in Fig. 4 indicate the results of linear fits in the high-temperature range, from which corresponding activation energies are determined. At a low-excitation density, the results yield spatially averaged activation energies of 325 ± 15 and 255 ± 9 meV for the GS and first excited-state transitions, respectively. Activation energies of the ground and first excited states obtained at low excitation in the 230–300-K temperature range for the QD samples used in this study are summarized in Table II. The difference between activation energies of the first excited state and the ground state, $\Delta E_{A10} = E_{A1} - E_{A0}$, is close to the intersublevel spacing (i.e., the difference in transition energies between these states, $\Delta E_{10} = E_1 - E_0$). The measured activation energies can be used to help deduce the physical process of carrier reemission and distinguish between the three general cases of reemission involving excitons, correlated electron–hole pairs, and independent single carriers. The reemission of correlated electron–hole pairs from the

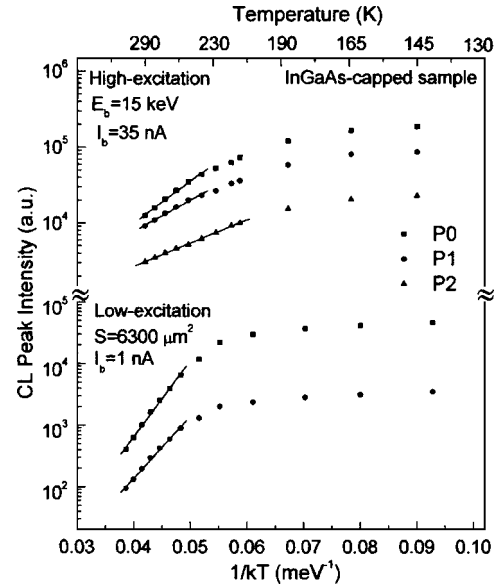


FIG. 4. A semilogarithmic plot of the spatially averaged CL intensities of the GS P0 and excited-state transitions, P1 and P2, for the InGaAs-capped sample vs $1/kT$ under low- and high-excitation conditions, which exhibit an Arrhenius behavior. The e-beam was sharply focused under high-excitation conditions, whereas the e-beam was uniformly defocused to a circular spot having an area of $\sim 6300 \mu\text{m}^2$ under low-excitation conditions. The solid lines indicate the results of linear fits in the temperature range of 230–300 K, from which corresponding activation energies are determined, as shown. As can be seen, activation energies of the ground and first excited states are significantly reduced at high excitation relative to their values at low excitation.

QD states to the barrier is possible in the strong confinement regime, when Coulomb-induced electron–hole correlations are weak.³³ If carriers are reemitted as correlated electron–hole pairs, then according to the requirement of detailed balance, the measured activation energy would be about half of the total barrier height.³⁴ The difference between activation energies of the first excited state and the ground state would be about half of the difference in transition energies between these states.³⁴ For the case of exciton reemission, the activation energy would be approximately equal to the barrier height, and the difference between activation energies of the first excited state and the ground state would be close to the difference in transition energies between these states.³⁴ Finally, if carriers are reemitted independently, the measured activation energy would be determined by the activation energy of the more weakly bound carrier-type (i.e., most probably the hole) and would be less than half of the total barrier height.^{25,35,36} In this case, the difference between activation

TABLE II. Activation energies of the ground (E_{A0}) and the first excited states (E_{A1}) obtained at low-excitation densities in the 230–300-K range for the InAs QD samples used in this study. Note that $\Delta E_{A10} = E_{A1} - E_{A0}$ and $\Delta E_{10} = E_1 - E_0$.

	E_{A0} (meV)	E_{A1} (meV)	ΔE_{A10} (meV)	ΔE_{10} (meV)
Sample 1	306 ± 10	219 ± 6	87	87
Sample 2	306 ± 12	235 ± 8	71	71
Sample 3	315 ± 9	251 ± 7	64	67
InGaAs-capped	325 ± 15	255 ± 9	70	67
GaAs-capped	300 ± 8	232 ± 7	68	73

energies of the first excited state and the ground state would be also less than half of the difference in transition energies between these states.^{35,36} The total barrier height depends on whether the reemission is to the WL or to the GaAs barrier; it is equal either to $\Delta E_B = E_{WL} - E_i$ or to $\Delta E_B = E_{GaAs} - E_i$, where E_{WL} , E_{GaAs} , and E_i are the transition energies of the wetting layer (WL), GaAs barrier, and the i th QD state.³⁴ The WL and GaAs emission energies, E_{WL} and E_{GaAs} , are ~ 1.420 and 1.510 eV, respectively, at $T \approx 100$ K.^{8,37} Our experimental results in Table II show activation energies that are too large to be consistent with the reemission of single carriers or correlated pairs. Within the margins of error ($\sim 10\% - 15\%$) the derived activation energies are quite close to the exciton localization energies with respect to the WL.¹⁵⁻¹⁷ Moreover, the measured difference between activation energies of the first excited state and the ground state for each of the five samples is close to the difference in transition energies between these states, which is also consistent with the inferred process of exciton reemission. Therefore, the magnitudes of the measured activation energies together with the approximately equal differences between transition and activation energies of the ground and first excited states (i.e., $\Delta E_{A10} \approx \Delta E_{10}$) demonstrate that dissociation of both ground- and excited-state excitons from the QD states into the WL (i.e., exciton emission) is responsible for the observed temperature dependence of the luminescence in the $\sim 230 - 300$ -K range at low excitation.

In previous studies, the dependence of the integrated PL intensity of the GS transition on excitation density was measured at low-excitation densities and different temperatures for InAs/GaAs QD samples.¹⁸ The behavior was purely linear at low temperatures, while at temperatures above ~ 250 K a superlinear, nearly quadratic behavior, was observed.¹⁸ In order to explain the observed behavior, a model based on an independent capture and escape of electrons and holes was proposed.¹⁸ At low excitation when much less than one electron-hole pair per dot is available, the probability that one electron and one hole are captured in the same QD depends quadratically on the excitation density. As the average occupation becomes higher than one electron-hole pair per dot this probability will vary linearly with excitation. No such excitation-dependent studies have been previously reported for excited-state transitions in QD samples. In order to investigate this further, the spatially averaged CL intensity of the ground-state (P0) and first excited-state (P1) transitions was measured in the $250 \leq T \leq 300$ K temperature range versus beam currents I_b in the range of 100 pA– 10 nA for a beam-broadened excitation area of $S = 6300 \mu\text{m}^2$, which enables detection in the limit of very low excitation. A linear regression of the log-log plots of CL intensity for P0 and P1 vs I_b resulted in slopes k of 1 ± 0.05 for all samples in this high-temperature range, reflecting a linear dependence of intensity on excitation density. We deduce from these results that carriers are captured as excitons or correlated e-h pairs. This is entirely consistent with the notion that exciton emission is the primary process for escape, as determined from the activation energy data previ-

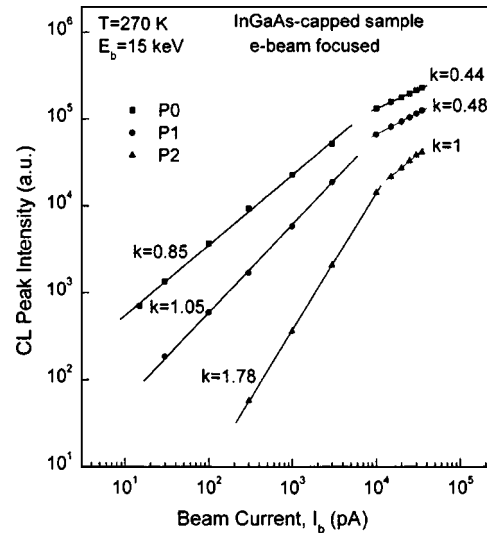


FIG. 5. Log-log plot of the spatially averaged CL intensity of the GS P0 and two excited-state transitions, P1 and P2, vs beam current at intermediate and high-excitation densities for the InGaAs-capped sample. The solid lines are linear regressions. A slope of $k=1$ reflects a linear dependence. Slopes larger than 1 represent a superlinear dependence. Slopes smaller than 1 are attributed to state filling of the QD and the WL states and represent a sublinear dependence.

ously discussed. For comparison, a quadratic dependence would have yielded $k=2$ and would have implied an independent carrier capture mechanism.¹⁸

C. State-filling effects in QDs

A log-log plot of the spatially averaged CL intensity of the GS P0 and two excited-state transitions, P1 and P2, versus beam current at intermediate and high-excitation densities are shown in Fig. 5 for the InGaAs-capped sample. The focused electron beam was rastered over a $64 \times 48 \mu\text{m}^2$ region with various probe currents in the $0.03 \leq I_b \leq 40$ nA range. The solid lines are linear regressions with slopes k indicated in the figure. A slope of $k=1$ corresponds to a linear dependence, where carriers are captured into QD states in the form of correlated electron-hole pairs or excitons.¹⁸ Slopes larger than 1 represent a superlinear dependence and reflect the capture of independent electrons and holes into QD states.¹⁸ Slopes smaller than 1 are attributed to an excitation regime where state filling of the QDs and the WL occurs and represent a sublinear dependence. A sublinear dependence with $k=0.85$ is observed for the intensity of the GS transition P0 begins to saturate at relatively low beam currents, $I_b \geq 0.5$ nA, when a steady-state average occupation in the QDs is already about two electron-hole pairs per dot, from Eq. (1). An additional decrease in the slope k is observed for beam currents above 10 nA, due to state filling of the WL. It is commonly believed that the WL acts as a barrier for the carrier capture and thermal escape processes.^{8,15-17} The slope k of P1 remains equal to 1 for beam currents below 10 nA. At higher beam currents saturation of the intensity of the first excited-state transition begins and a sublinear behavior is observed. A markedly different behavior is revealed for emission of the second excited-state

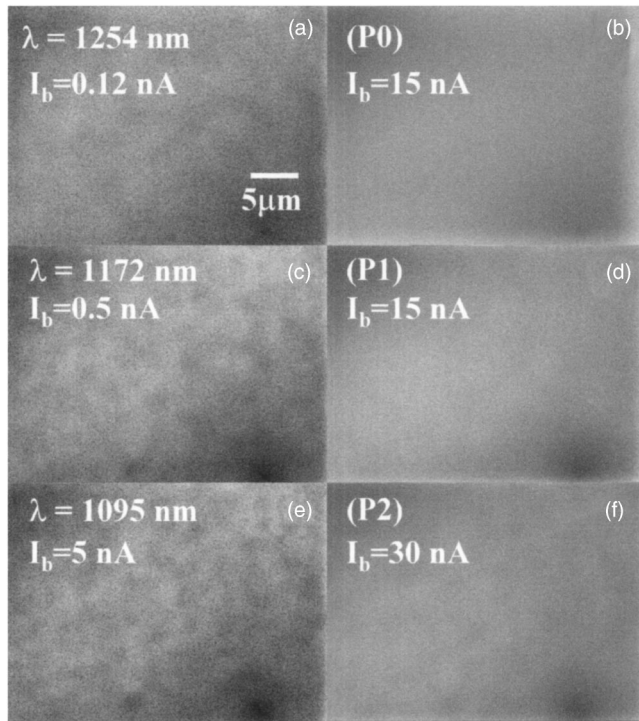


FIG. 6. A set of monochromatic CL images at low and high excitations (as indicated) that were obtained while an electron beam of $E_b=15$ keV was rastered over a $32 \times 24 \mu\text{m}^2$ region for the InGaAs-capped sample at $T=190$ K: (a) and (b) represent CL images of the GS component at the peak wavelength $\lambda_m=1254$ nm; (c) and (d) and (e) and (f) represent CL images of the first and second excited-state components acquired at peak wavelengths of $\lambda_m=1172$ nm and $\lambda_m=1095$ nm, respectively. Increasing the excitation density results in a *spatial smearing effect*.

P2. For beam currents below 15 nA, a superlinear dependence is observed, while at higher excitations the behavior becomes linear or sublinear. This behavior is consistent with the independent capture and filling of electrons and holes in excited states at low excitations and high temperatures where the probability of a correlated electron-hole pair being captured simultaneously into higher excited states is much less than 1.¹⁸ Similar results are obtained for the other four samples.

A set of monochromatic CL images that were acquired at wavelengths corresponding to the GS and two excited-state transitions in QDs at low- and high-beam currents are shown in Fig. 6 over a $32 \times 24 \mu\text{m}^2$ region of the InGaAs-capped sample. The monochromatic CL images in Figs. 6(a), 6(c), and 6(e) were acquired with beam currents in which state-filling effects were negligible (see Fig. 6). In contrast, CL images in Figs. 6(b), 6(d), and 6(f) were acquired for beam currents corresponding to a strong saturation of CL intensities of the GS and excited-state transitions. Monochromatic CL images of the ground and excited QD states acquired at low-excitation densities reveal spatial variation in the intensity of luminescence, with domain sizes on the order of $\sim 1 \mu\text{m}$. At higher excitations, a nearly uniform spatial distribution of the CL intensities is observed. Thus, an increase in excitation density to a level that approaches saturation of a particular QD state results in a spatial smearing effect. The

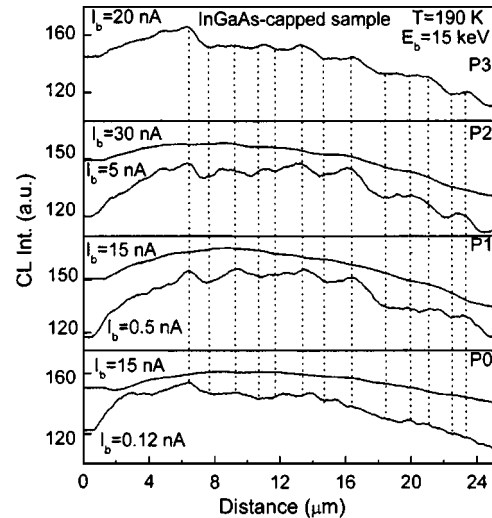


FIG. 7. Line-scan analysis for the InGaAs-capped sample at $T=190$ K showing the CL intensity of the GS P0 and excited-state transitions P1–P3 at low- and high-excitation conditions vs distance along an arbitrary line. The vertical dashed lines illustrate the spatial correlation between peaks and dips of this scans. Spatial smearing occurs for large excitations due to an equilibration of carrier populations in adjacent groups of QDs.

monochromatic CL image acquired for the third excited state is not shown here, owing to its similarity in behavior with the other CL images.

In order to analyze the spatial correlations between CL of the GS and three excited-state transitions and better understand the existing spatial variations of CL, a binning of pixels along an arbitrary horizontal line in the images of Fig. 6 was performed. As a result, a plot of the CL intensity versus linear distance is shown in Fig. 7. The strong correlation of the dips and peaks, as illustrated by the vertical dashed lines, indicates that the GS P0 and excited-state peaks (P1, P2, and P3) stem from the same QDs. At low-excitation densities, a noticeable spatial variation (i.e., contrast in the images) of $\sim 15\%$ in the CL intensity of the GS and three excited-state transitions is observed. The intensity variations are likely caused by changes in the sizes of groups of QDs and spatial variations in thermally induced reemission of carriers, as previously established by CL wavelength imaging of similar SAQD samples.¹⁹ Spatial smearing occurs for large excitations due to an equilibration of carrier populations in adjacent groups of QDs, as illustrated in Fig. 8. At low-excitation densities, the QD emission is dominated by the GS emission of larger QDs that have smaller transition energies.

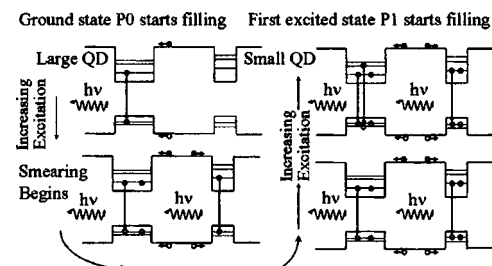


FIG. 8. Schematic illustration of successive state filling in adjacent groups of QDs resulting in an equilibration of carrier populations and an excitation-dependent *spatial smearing effect*.

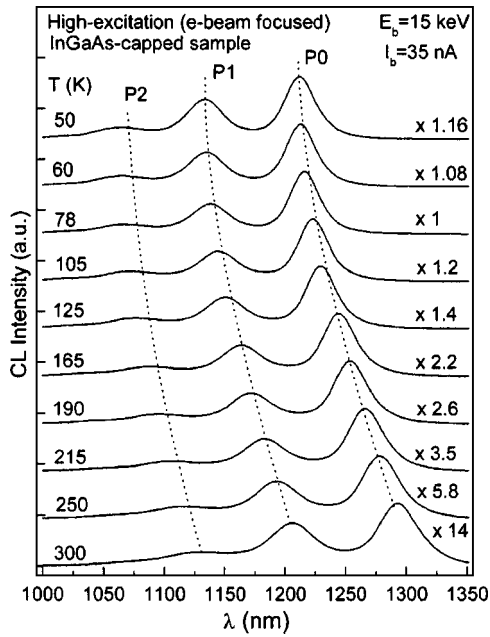


FIG. 9. Spatially averaged CL spectra of the InGaAs-capped sample acquired under a high-excitation condition where $I_b=35$ nA in the $50 \leq T \leq 300$ K range. The GS P0 and two excited-state peaks, P1 and P2, are indicated.

A much weaker emission of the first excited state is also observed, as seen in Figs. 1 and 2. On increasing the excitation density, the GS emission of larger QDs saturates when a steady-state average occupation in these QDs is already about two electron-hole pairs per dot, and a subsequent filling of smaller QDs begins. This is followed by an equilibration of the carrier populations in adjacent groups of larger and smaller QDs, which in turn causes a simultaneous decrease in the spatial variation of the intensity of the GS transition, thereby causing the observed spatial smearing effect. As we increase the excitation density still further, a filling of the first excited state of larger QDs begins, as shown in Fig. 2. The carriers will then begin to fill the first excited state in groups of larger QDs until its saturation induces carriers to begin filling the first excited state in groups of smaller QDs. The process will continue for filling of the P1 state in the same manner as described for the filling of the GS P0 state. Thus, as the excitation is increased, a sequential filling of the GS P0, P1, and P2 states occurs in which spatial smearing is caused by an equilibration of carrier density between the states in adjacent groups of larger and smaller QDs.

D. Temperature-dependent CL and thermalization in QDs at high excitations

Spatially averaged CL spectra of the InGaAs-capped sample were acquired while the focused electron beam was rastered over a $64 \times 48 \mu\text{m}^2$ region for a beam energy of 15 keV and beam current of 35 nA, as shown in Fig. 9. At this excitation, the CL intensities of the GS and two excited-state transitions are strongly saturated. Spectra were acquired for various temperatures in the 50–300-K temperature range. All the spectra are normalized to have nearly the same intensity, and the scaling factors are indicated.

TABLE III. Activation energies of the ground (E_{A0}) and two excited states (E_{A1} and E_{A2}) obtained at high-excitation density in the 230–300-K range for the InAs QD samples used in this study.

	E_{A0} (meV)	E_{A1} (meV)	E_{A2} (meV)
Sample 1	190 ± 3	160 ± 8	154 ± 6
Sample 2	189 ± 4	150 ± 1	150 ± 1
Sample 3	187 ± 11	147 ± 9	135 ± 8
InGaAs-capped	186 ± 10	145 ± 11	135 ± 8
GaAs-capped	184 ± 12	163 ± 13	158 ± 7

A semilogarithmic plot of the spatially averaged CL intensity of the GS and two excited-state transitions versus $1/kT$ at high excitation is shown in the upper part of Fig. 4 for these spectra. The solid lines indicate the results of linear fits in the 230–300-K temperature range, from which corresponding activation energies are determined. The results yield spatially averaged activation energies of 186 ± 10 , 145 ± 11 , and 135 ± 8 meV for the ground and two excited-states, respectively. It is apparent from Fig. 4 that the activation energies of the ground and the first excited states are significantly reduced at high excitation relative to their values of 325 ± 15 and 255 ± 9 meV at a low-excitation density. Activation energies measured under this high-excitation density in the 230–300-K temperature range for the five QD samples are listed in Table III. We assume that at high-excitation densities the WL states are filled and the decrease in the QD emission with increasing temperature in the 230–300-K temperature range is attributed to thermal escape of less-confined carriers from respective QD states into the GaAs barrier.¹⁸ Although an uncertainty exists in the band offset ratio for the InAs QDs, several authors have pointed out that the hole-confinement energy ΔE_h is weaker than the electron confinement energy ΔE_e for lens-shaped QDs.^{25,35,36} The ground-state activation energies (see Table III) are comparable with a value for the ground-state hole localization energy with respect to the GaAs barrier, as calculated for a lens-shaped InAs QD and equal to 193 meV.³⁸ Assuming that the measured activation energies of the ground and excited states are equal to the barrier heights of the holes with respect to the GaAs barrier, we can extract the ratio of localization energies from

$$Q_L = E_{Ai}/(E_{\text{GaAs}} - E_i), \quad (2)$$

where E_{Ai} and E_i are the activation and transition energies for the i th QD state. We obtain values of the ratio of localization energies in the range of $\sim 33\% - 38\%$. These values are in good agreement with other values reported in the literature.¹⁸ We expect that these values for Q_L are also close to the hole-band offset ratio. Such consistency further suggests strongly that thermal reemission of single holes into the GaAs barrier is indeed responsible for the observed temperature dependence of the CL intensity of the GS P0 and two excited-state, P1 and P2, transitions in the ~ 230 –300-K temperature range for high-excitation conditions. This is to be compared with the excitonic nature of carrier reemission under low-excitation conditions, as discussed in Sec. III B.

IV. SUMMARY AND CONCLUSIONS

We have examined in detail the optical properties of self-assembled InAs QDs with cathodoluminescence (CL) imaging and spectroscopy under various excitation conditions and sample temperatures. The InAs QDs were formed via self-assembly during MBE growth of InAs on undoped planar GaAs (001). The CL images and spectra revealed the ground state (GS) and up to three QD excited states. A suppressed relaxation (i.e., the phonon bottleneck effect) from the first excited state at very low excitation density was observed. The excitation density dependence of the CL intensity of the ground and first excited-state transitions was shown to be linear at all temperatures for low-excitation conditions. This result can be understood by considering that carriers (i) are captured as excitons or correlated electron-hole pairs and (ii) escape via thermal reemission as excitons. At sufficiently high excitations, state-filling and spatial smearing effects are observed together with a sublinear dependence of the CL intensity on excitation density. We present a simple model to explain the spatial smearing effect. A successive filling of the ground and excited states in adjacent groups of QDs having different size distributions is proposed to be the cause of spatial smearing under high-excitation conditions. The CL intensities of the ground- and excited-state transitions were analyzed as a function of temperature and excitation to study the thermal activation and reemission of carriers. Thermal quenching of the CL intensity of the QD ground- and first excited-state transitions at low excitation in the ~ 230 – 300 -K temperature range is attributed to dissociation of excitons from the QD states into the WL (i.e., a reemission of excitons). At high-excitation conditions, significant reductions in the activation energies of the ground and excited states are found. This suggests strongly that the thermal reemission of single holes from QD states into the GaAs barrier is responsible for the observed temperature dependence of the QD luminescence in the ~ 230 – 300 -K temperature range. An improved understanding of the operation and design of InAs/GaAs QD-based optoelectronics could emanate from these results and other optical studies involving the excitation and temperature dependence of such samples.

ACKNOWLEDGMENTS

This work was supported by the Israel Science Foundation and by the DoD Multidisciplinary University Research Initiative (MURI) program administrated by AFOSR.

¹N. Kirstaedter *et al.*, Appl. Phys. Lett. **69**, 1226 (1996).

²L. Chu, A. Zrenner, M. Bichler, and G. Abstreiter, Appl. Phys. Lett. **79**, 2249 (2001).

³Z. Chen, E.-T. Kim, and A. Madhukar, Appl. Phys. Lett. **80**, 2490 (2002).

⁴J. J. Finley, M. Skaltitz, M. Arzberger, A. Zrenner, G. Böhm, and G.

Abstreiter, Appl. Phys. Lett. **73**, 2618 (1998).

⁵M. C. Bödefeld, R. J. Warburton, K. Karrai, J. P. Kotthaus, G. Medeiros-Ribeiro, and P. M. Petroff, Appl. Phys. Lett. **74**, 1839 (1999).

⁶T. Lundstrom, W. Schoenfeld, H. Lee, and P. M. Petroff, Science **286**, 2312 (1999).

⁷Z. Y. Xu *et al.*, Phys. Rev. B **54**, 11528 (1996).

⁸Y. Tang, D. H. Rich, I. Mukhametzanov, P. Chen, and A. Madhukar, J. Appl. Phys. **84**, 3342 (1998).

⁹S. Fafard *et al.*, Surf. Sci. **361**, 778 (1996).

¹⁰Y. T. Dai, J. C. Fan, Y. F. Chen, R. M. Lin, S. C. Lee, and H. H. Lin, J. Appl. Phys. **82**, 4489 (1997).

¹¹K. Mukai, N. Ohtsuka, and M. Sugawara, Appl. Phys. Lett. **70**, 2416 (1997).

¹²Y. Wu, K. Arai, and T. Yao, Phys. Rev. B **53**, R10485 (1996).

¹³A. Patane, A. Polimeni, P. C. Main, M. Henini, and L. Eaves, Appl. Phys. Lett. **75**, 814 (1999).

¹⁴W.-H. Chang, T. M. Hsu, C. C. Huang, S. L. Hsu, C. Y. Lai, N.-T. Yeh, and J.-I. Chyi, Phys. Status Solidi B **224**, 85 (2001).

¹⁵R. Heitz, I. Mukhametzanov, H. Born, M. Grundmann, A. Hoffmann, A. Madhukar, and D. Bimberg, Physica B **272**, 8 (1999).

¹⁶R. Heitz, I. Mukhametzanov, A. Madhukar, A. Hoffmann, and D. Bimberg, J. Electron. Mater. **28**, 520 (1999).

¹⁷W.-H. Chang, T. M. Hsu, N.-T. Yeh, and J.-I. Chyi, Chin. J. Phys. (Taipei) **40**, 548 (2002).

¹⁸E. C. Le Ru, J. Fack, and R. Murray, Phys. Rev. B **67**, 245318 (2003).

¹⁹D. H. Rich, C. Zhang, I. Mukhametzanov, and A. Madhukar, Appl. Phys. Lett. **76**, 3597 (2000).

²⁰U. Bockelman and G. Bastard, Phys. Rev. B **42**, 8947 (1990).

²¹H. Benisty, C. M. Sotomayor-Torres, and C. Weisbuch, Phys. Rev. B **44**, 10945 (1991).

²²R. Heitz, H. Born, F. Guffarth, O. Stier, A. Schliwa, A. Hoffmann, and D. Bimberg, Phys. Rev. B **64**, 241305 (2001).

²³K. Mukai, N. Ohtsuka, H. Shoji, and M. Sugawara, Phys. Rev. B **54**, R5243 (1996).

²⁴S. Raymond *et al.*, Phys. Rev. B **54**, 11548 (1996).

²⁵M. Grundmann, N. N. Ledentsov, O. Stier, D. Bimberg, V. M. Ustinov, P. S. Kop'ev, and Zh. I. Alferov, Appl. Phys. Lett. **68**, 979 (1996); M. Grundmann, N. N. Ledentsov, O. Stier, J. Böhrer, D. Bimberg, V. M. Ustinov, P. S. Kop'ev, and Zh. I. Alferov, Phys. Rev. B **53**, R10509 (1996).

²⁶H. Lee, W. Yang, and P. C. Sercel, Phys. Rev. B **55**, 9757 (1997).

²⁷F. Pulizzi, A. J. Kent, A. Patanè, L. Eaves, and M. Henini, Appl. Phys. Lett. **84**, 3046 (2004).

²⁸E.-T. Kim, Z. Chen, and A. Madhukar, Appl. Phys. Lett. **81**, 3473 (2002).

²⁹H. T. Lin, D. H. Rich, A. Konkar, P. Chen, and A. Madhukar, J. Appl. Phys. **81**, 3186 (1997).

³⁰U. Jahn, S. Dhar, O. Brandt, H. T. Grahn, and K. H. Ploog, J. Appl. Phys. **93**, 1048 (2003).

³¹R. Heitz, F. Guffarth, I. Mukhametzanov, M. Grundmann, A. Madhukar, and D. Bimberg, Phys. Rev. B **62**, 16881 (2000).

³²E. T. Kim, Z. H. Chen, and A. Madhukar, Appl. Phys. Lett. **79**, 3341 (2001).

³³G. W. Bryant, Phys. Rev. B **37**, 87633 (1988).

³⁴W. Yang, R. R. Lowe-Webb, H. Lee, and P. C. Sercel, Phys. Rev. B **56**, 13314 (1997).

³⁵W.-H. Chang, T. M. Hsu, C. C. Huang, S. L. Hsu, C. Y. Lai, N. T. Yeh, T. E. Nee, and J.-I. Chyi, Phys. Rev. B **62**, 6959 (2000).

³⁶R. Collombelli, V. Piazza, A. Badolato, M. Lazzarino, F. Beltram, W. Schoenfeld, and P. Petroff, Appl. Phys. Lett. **76**, 1146 (2000).

³⁷W.-H. Chang, W. Y. Chen, T. M. Hsu, N.-T. Yeh, and J.-I. Chyi, Phys. Rev. B **66**, 195337 (2002).

³⁸A. J. Williamson, L.-W. Wang, and A. Zunger, Phys. Rev. B **62**, 12963 (2000).